On the Interdependence of AC-Side and DC-Side Optimum Control of Three-Phase Neutral-Point-Clamped (Three-Level) PWM Rectifier Systems

JOHANN W. KOLAR, UWE DROFENIK, FRANZ C. ZACH

Technical University Vienna, Power Electronics Section 359.5
Gusshausstraße 27, Vienna A-1040, Austria/Europe
Tel.: +43-1-58801-3833 Fax.: +43-1-505 88 70
e-mail: kolar@ps1.iaee.tuwien.ac.at

Abstract. Three-phase neutral point clamped (three-level) PWM rectifier systems show redundant switching states concerning the formation of the local average values of the line-to-line input voltages. Therefore, time-weighting of these switching states represents a degree of freedom of the control of these systems which usually is applied for balancing the DC link capacitor voltages. However, proper weighting of the redundant switching states also can be used for a minimization of the rms value of the mains current harmonics or for a minimization of the load of the capacitive center point of the output voltage. Therefore, in connection with an optimization of the control of the systems the following question (which has not been analyzed in literature so far) has to be posed: (i) with which increase of the load on the output capacitors one has to pay for the optimization of the mains-side operating behavior or, vice versa, (ii) to which extent does a minimization of the load on the capacitors contribute to an increase of the ripple of the mains current. In this paper for resistive fundamental mains behavior (sinusoidal mains current shape), constant output voltage and high pulse frequency, via analytical calculations and digital simulations the optimization of the AC-side or DC-side operational behavior is analyzed in detail. This yields the calculation of the local time-weighting of the redundant switching states in dependency of the modulation depth for minimum local rms value of the mains current harmonics and minimum local average value of the neutral point current. Based on this, for AC-side optimal and DC-side optimal and for a suboptimal case the global rms value of the mains current harmonics and the low-frequency harmonics of the center point current are calculated in dependency on the modulation depth and a comparison of the different control methods is given. Finally, the time shapes of the modulation functions and of the zero-sequence component of the input phase voltages of the systems are determined as they are related to the different optimal control methods. This gives a basis for a control of the voltage formation via a subharmonic oscillation method as alternative to a space vector oriented control of the systems.

Keywords. Three-phase neutral-point-clamped (three-level) PWM converter systems, optimization of AC-side or DC-side operational behavior, control of neutral point potential.

1 Introduction

Neutral-point-clamped or three-level PWM rectifier systems [1]–[6] are characterized by inclusion of the center point of the output voltage into the circuit topology. As compared to two-level converters, this leads to reduced rms values of the harmonics with switching frequency of the sinusoidally controlled mains current and to lower blocking voltage stress on the valves (cf. p. 518 in [2]). For avoiding a potential shift of the capacitive output voltage center point (neutral point) one has to provide, however, also a symmetrization of the output partial voltages besides controlling the overall output voltage. For this purpose switching states of the systems are used which are redundant with respect to the line-to-line voltage formation on the AC side but which lead to opposite signs of the current which is fed into the neutral point [7], [8] . Via appropriate time-weighting of the switching states which are present in each case at the begin and end of a pulse half period the local average value of the center point current can be adjusted and thereby the potential of the center point can be controlled. There, the voltage space vector being formed in the average over a pulse period at the input of the rectifier system is not influenced. Therefore, independently of the specific distribution of the redundant switching states between begin and end of a pulse half period a sinusoidal guidance of the mains current is given.

If now all non-ideal properties of a practical circuit are neglected, a control of the voltage distribution could be omitted theoretically in the stationary case. Therefore, the question should be posed whether in this case the distribution of the redundant switching states can be selected such that an optimization criterion characterizing the operational behavior or the load on a component of the power circuit is led to an optimum. The overall duration (to be distributed by the optimization) of the redundant switching states is given there by the absolute value and phase of the voltage space

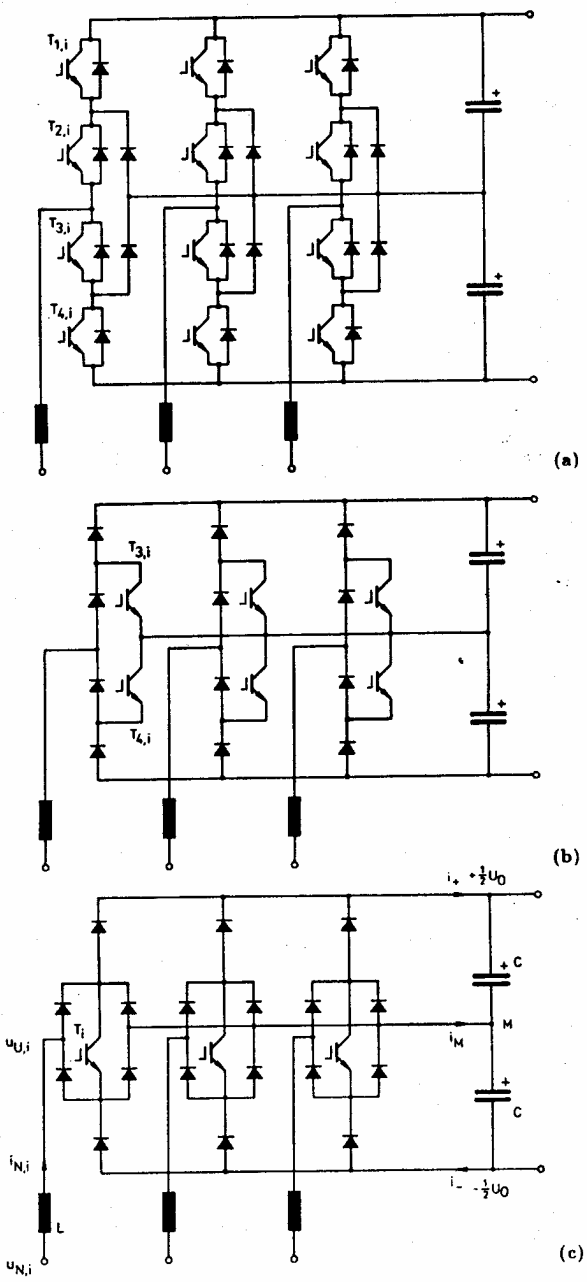

Fig.1: Basic structure of the power circuits of three-phase PWM rectifier systems. (a): bidirectional PWM rectifier system according to [2] (for $u_{U,i} = +\frac{1}{2}U_O$ the transistors $T_{1,i}$ and $T_{2,i}$ are turned on within a bridge leg i; also, transistors $T_{2,i}$ and $T_{3,i}$ for $u_{U,i} = 0$ and transistors $T_{3,i}$ and $T_{4,i}$ for $u_{U,i} = -\frac{1}{2}U_O$); (b): unidirectional three-level PWM rectifier system according to [5] (the phase voltages $u_{U,i} = +\frac{1}{2}U_O$ and $u_{U,i} = -\frac{1}{2}U_O$ are formed during the off-time of the power transistors $T_{3,i}$ and $T_{2,i}$ in dependency on the sign of the related phase current $i_{N,i}$, $u_{U,i} = 0$ is obtained by turning on $T_{3,i}$ and $T_{2,i}$); (c): VIENNA rectifier (unidirectional) according to [6] (voltage formation as for (b), in each phase the switching elements $T_{3,i}$ and $T_{2,i}$ of the circuit shown in (b) are replaced by a bidirectional bipolar switching element T_i).

vector which has to be formed in the average over a considered pulse interval. This overall duration also can be given by the modulation depth and the position of the pulse interval within a mains period. Besides the voltage formation as further (only marginally constraining) side condition of the optimization a symmetry of the control of the single phase legs has to be provided which avoids the occurrence of a DC component of the center point current.

Within the scope of this paper the possibility of an optimization of the AC-side and DC-side operational behavior of unidirectional and bidirectional three-level PWM rectifier systems (cf. **Fig.1**) is investigated. For the considerations resistive mains fundamental behavior, i.e. a sinusoidal shape of the phase currents in phase with the related phase voltages, constant output voltage and constant pulse frequency of the systems are assumed. Because with these assumptions all rectifier systems shown in Fig.1 have equal stationary operating behavior, the considerations are limited to the system with the simplest structure (cf. Fig.1(c)) for the sake of clearness. Based on an analysis of the voltage formation of the system in **section 2** the redundancy of system switching states is verified and the possibility to influence the AC-side and/or DC-side operational behavior by changing the distribution of the redundant switching states is analyzed. In **section 3** as quality index of an optimization of the distribution the local rms value (related to a pulse period) of the mains current harmonics and the absolute value of the local average value of the center point current are defined. Both quality criteria are chosen with respect to a maximization of the power density of the system. By minimization of the mains current harmonics for given switching frequency the rated power of the inductances connected in series on the mains side are utilized optimally concerning a reduction of the effects on the mains caused by the system. Via minimization of the local load of the output voltage center point the avoidance and/or limitation of the low-frequency components of the center point current is strived for. This reduces the capacity value of the output capacitors and allows to replace electrolytic capacitors by foil capacitors with higher life time. In **section 4**, the optimum distributions of the redundant switching states (resulting for the AC and DC side optimizations) are calculated by digital simulations in dependency on the position of the considered pulse interval within a mains period and the given modulation depth. The considerations lead to a suboptimal control method which is characterized by a simple realization and which corresponds to a great extent to the AC-side optimization of the system operating behavior. Furthermore, the global rms value of the mains current harmonics (related to the fundamental) and the low-frequency harmonics of the center point current resulting for optimal and suboptimal choice of the distribution of the redundant switching states are calculated in dependency on the modulation depth and compared. In **section 5** the time shapes of the local average values of the input phase voltages (characterizing the different optimal control methods) and the zero quantity of the phase voltages are calculated. They can be used as basis for the control of the system via a subharmonic oscillation method. Finally, in **section 6** the inclusion of the control of the potential of the output voltage center point into the optimum control methods will be discussed.

2 Basic Considerations

In the following the voltage formation of three-level converter systems is analyzed briefly. The free parameter which makes possible the optimization of the operating behavior of the system is determined. Then, in sections 2.3 and 2.4 the possibility of influencing the AC-side and DC-side operating behavior of the systems by modification of the voltage control is discussed.

2.1 Control of the Rectifier Input Voltage

The bidirectional three-level converter system shown in **Fig.1(a) has 3** admissible switching states for each bridge leg, resulting in a total of $3^3 = 27$ possible switching states. To these switching states the space vectors $\underline{u}_{U,j}$ of the rectifier input phase voltages $u_{U,i}$, $i = R, S, T$ are related as given in **Fig.2**. For the denomination of the voltage space vectors one can use the relevant combination of signs of the voltages $u_{U,i}$ (as related to the center point M of the output voltage). There, for connecting the AC terminal of a bridge leg with M the value 0 is inserted according to $u_{U,i} = 0$.

For purely rectifier operation and/or for unidirctional energy conversion the number of turn-off power semiconductors (and, therefore, also the system complexity) can be reduced as explained in [5] and [6] and as shown in **Fig.1(b)** and **(c)**. However, this limits also the system controllability because now besides the switching function s_i of a bridge leg also the $\mathrm{sign}\{i_{N,i}\}$ of the related phase current influences the voltage formation

$$u_{U,i} = \begin{cases} \mathrm{sign}\{i_{N,i}\}\frac{U_O}{2} & \text{if } s_i = 0 \\ 0 & \text{if } s_i = 1 \,. \end{cases} \qquad (1)$$

Besides $u_{U,i} = 0$ by each bridge leg only $u_{U,i} = +\frac{1}{2}U_O$ or $u_{U,i} = -\frac{1}{2}U_O$ can be generated therefore. For each combination of signs of the phase currents therefore only $2^3 = 8$ phase voltage triples $(u_{U,R}, u_{U,S}, u_{U,T})$ are available for the formation of a given space vector $\underline{u}_U^*$. To these triples voltage space vectors are associated which point into the corner points and into the center point of a hexagonal sector of the space vector plane. The angular position of the hexagonal area is defined by the signs of the phase currents $i_{N,i}$ and/or by the phase φ_N of the mains current space vector $\underline{i}_N$. E.g., the sign combination $\mathrm{sign}\{i_{N,R}\} = +1$, $\mathrm{sign}\{i_{N,S}\} = -1$, $\mathrm{sign}\{i_{N,T}\} = -1$ and/or the angle interval $\varphi_N \in (-\frac{\pi}{6}, +\frac{\pi}{6})$ is associated to the hexagonal area pointed out by the dotted area in Fig.2 [9]. When $\underline{i}_N$ enters the next following angle or sign interval $\varphi_N \in (+\frac{\pi}{6}, +\frac{\pi}{2})$ (the sign of $i_{N,S}$ is changed to $\mathrm{sign}\{i_{N,S}\} = +1$), the hexagon defining the realizable voltage space vectors is turned by an angle of $\frac{\pi}{3}$; the voltage space vectors again will lie symmetrically around the median line of the $\frac{\pi}{3}$-wide angle region φ_N.

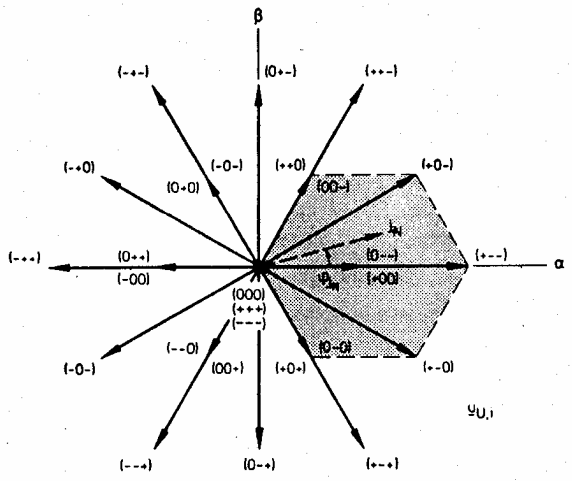

Fig.2: Voltage space vectors of the bidirectional three-level PWM rectifier system according to Fig.1(a). For the denomination of the space vetors the relevant combinations of signs of the phase voltages $u_{U,i}$ (as related to the center point M of the output voltage) are used; there, for connecting the AC terminal of a bridge leg with M the value 0 is inserted according to $u_{U,i} = 0$. The hexagon defining the realizable voltage space vectors of unidirectional three-level rectifier systems according to Figs.1(b) and (c) for $\mathrm{sign}\{i_{N,R}\} = +1$, $\mathrm{sign}\{i_{N,S}\} = -1$, $\mathrm{sign}\{i_{N,T}\} = -1$ and/or the angle interval $\varphi_N \in (-\frac{\pi}{6}, +\frac{\pi}{6})$ is pointed out by the dotted area.

In connection with a further analysis of the rectifier systems it is important to point out that despite of this significant limitation the space vector $\underline{u}_{U,j}$ (the index j denotes the switching state) being available for the relevant voltage generation one can obtain also for unidirectional systems a sinusoidal control of the mains current in phase with the mains voltage

$$\underline{u}_N = \hat{U}_N \exp j\varphi_N \,, \qquad \varphi_N = \omega_N t \,, \qquad (2)$$

(ω_N denotes the mains angular frequency) in the stationary case. This becomes clear by the following considerations: in order to obtain a purely sinusoidal mains current shape

$$\underline{i}_N^* = \hat{I}_N^* \exp j\varphi_N \,, \qquad (3)$$

we have to form a voltage space vector

$$\underline{u}_U^* = \hat{U}_U^* \exp j\varphi_U = \hat{U}_N \exp j\varphi_N - j\omega_N L \underline{i}_N^* \qquad (4)$$

at the input of the rectifier system in the average over a pulse period. By the space vectors $\underline{u}_U^* = \underline{u}_{U,(1)}$ and $\underline{i}_N^* = \underline{i}_{N,(1)}$ the fundamental component $u_{U,i,(1)}$ (with amplitude $\hat{U}_{U,(1)} = \hat{U}_U^*$) and $i_{N,i,(1)}$ (with amplitude $\hat{I}_{N,(1)} = \hat{I}_N^*$) of the phase quantities $u_{U,i}$ and $i_{N,i}$ are represented. Because for high pulse frequency the amplitude of the fundamental component $\omega_N L \underline{i}_N^*$ of the voltage drop across the series inductors L remains limited to a few percent of the mains voltage amplitude $\hat{U}_N$, $\underline{i}_N^*$ and/or the actually resulting mains current $\underline{i}_N$ and $\underline{u}_U^*$ have only a very small phase shift ($\varphi_U \approx \varphi_N$). Therefore, in the stationary case in a first approximation a voltage space vector $\underline{u}_U^*$ in the direction of the current space vector has to be generated. Therefore, the connection described here of the space vectors $\underline{u}_{U,j}$ (which are available for the voltage formation) with the angular position φ_N of $\underline{i}_N$ (as being characteristic for unidirectional systems) does not constitute a limitation of the stationary operating region for resistive mains behavior as compared to bidirectional systems.

If a sinusoidal current is impressed in phase with the mains voltage, the bidirectional rectifier system (according to Fig.1(a)) and the unidirectional systems according to Figs.1(b) and (c) show equal operating behavior,

therefore. An optimization of the stationary operation then basically can be limited to one system. Afterwards, it can be transferred directly to another system by appropriate recoding of the control inputs to the switching elements of the bridge legs. For the sake of clearness in the following the considerations will be related to the system of Fig.1(c), introduced in the literature as VIENNA rectifier system.

Remark: For scientific exactness one has to point out regarding the equivalence of considering the stationary operation of unidirectional and bidirectional PWM rectifier systems (with resistive mains behavior) that an ideal consistency is given only for negligible fundamental component of the voltage drop $\underline{u}_L$ across the series inductors and/or for (theoretically) infinitely high pulse frequency and/or for $\varphi_U \equiv \varphi_N$. A finite pulse frequency f_P leads (due to $\varphi_U < \varphi_N$) in connection with the current dependency of the voltage formation to a minor reduction of the control boundary of unidirectional systems (cf. Fig.4 in [9]). Furthermore, a discontinuous phase current behavior in the zero crossings occurs due to the partial replacement of bidirectional by unidirectional switching elements. However, for the conditions being typical for practical applications of the systems (namely for $\frac{f_P}{f_N} = 250 \ldots 1250$; f_N denotes the mains frequency) one can observe identical operating behavior for both systems with good approximation and, also, equal voltage control range in a first approximation.

2.2 Space Vector Modulation, Redundant Switching States and Degree of Freedom of the Voltage Control

Three-phase PWM rectifier systems show in general no connection of the DC-side circuit part with the mains star point (cf. Fig.1). The formation of the mains phase currents therefore is not influenced by a zero quantity

$$u_0 = \frac{1}{3}(u_{U,R} + u_{U,S} + u_{U,T}) \tag{5}$$

($u_{U,i} = u'_{U,i} + u_0$) contained in the phase voltages $u_{U,i}$. This is also a condition for a completely describable system behavior by space vector calculus because for formation of a voltage space vector

$$\underline{u}_U = \frac{2}{3}(u_{U,R} + \underline{a}\, u_{U,S} + \underline{a}^2 u_{U,T}) \qquad \underline{a} = \exp j\frac{2\pi}{3} \tag{6}$$

the zero quantity is decoupled according to

$$(1 + \underline{a} + \underline{a}^2)\, u_0 = 0\,. \tag{7}$$

Therefore, identical voltage space vectors are linked to switching states forming phase voltages which are only different concerning their zero quantity components. A pertinent redundancy of the switching states $j = (100)$ and (011) of the rectifier system according to Fig.1(c) becomes clear from **Fig.3**. (The switching state j of the rectifier system is marked by the quantity $j = (s_R, s_S, s_T)$ formed from the phase switching functions s_i; cf. Eq.(1).) There, the conditions for $i_{N,R} > 0$, $i_{N,S} < 0$ and $i_{N,T} < 0$ and/or for $\varphi_N \in (-\frac{\pi}{6}, +\frac{\pi}{6})$ are considered.

According to Eq.(4) one has to form a voltage space vector $\underline{u}_U^*$ which moves with constant angular speed on a circular trajectory with radius $\hat{U}_U^*$ in order to obtain an ideally sinusoidal shape $\underline{i}_N^*$ of the mains current. For the approximation of the ideally continuous motion of $\underline{u}_U^*$, basically 7 discrete voltage space vectors are available. The vector $\underline{u}_U^*$ therefore can be selected only on the basis of an average value over a pulse period ($\underline{u}_{U,\mathrm{avg}} = \underline{u}_U^*$). For obtaining a best possible approximation those space vectors are applied which are in the immediate vicinity of the vector tip, in each case. This is equivalent to using those switching states which are related to the corner points of that triangular region of the space vector plane into which the tip of the vector $\underline{u}_U^*$ points (marked in Fig.3 by a dotted area). Then there follows

$$\underline{u}_{U,\mathrm{avg}} = \underline{u}_U^* = \delta_{(100)}\underline{u}_{U,(100)} + \delta_{(000)}\underline{u}_{U,(000)} + \delta_{(010)}\underline{u}_{U,(010)} + \delta_{(011)}\underline{u}_{U,(011)} \tag{8}$$

for the vector $\underline{u}_U^*$ given in Fig.3. There, the weighting factors δ_j denote the relative on-time of the different switching states j. For a minimum system switching frequency the switching states within each pulse half period are arranged in such a way that consecutive states are obtained by switching of only one bridge leg. If one defines arbitrarily (100) as initial switching state, a switching state sequence

$$|_{t_\mu=0}(100)-(000)-(010)-(011)|_{t_\mu=\frac{1}{2}T_P}(011)-(010)-(000)-(100)|_{t_\mu=T_P} \tag{9}$$

results within each pulse period T_P, therefore. There, t_μ denotes a local time being counted within the pulse period. Due to the postulation of a minimum number of switchings one has to invert the sequence of the voltage vectors $\underline{u}_{U,j}$ after each pulse half period, therefore.

The weighting factors δ_j of the switching states $j = (000)$ and (010) can be calculated directly by evaluation of simple geometric relationships (cf. Fig.4 in [10]). There follows

$$\begin{aligned} \delta_{(000)} &= \sqrt{3}M\sin(\tfrac{\pi}{3} - \varphi_U) - 1 \\ \delta_{(010)} &= \sqrt{3}M\sin\varphi_U \end{aligned} \tag{10}$$

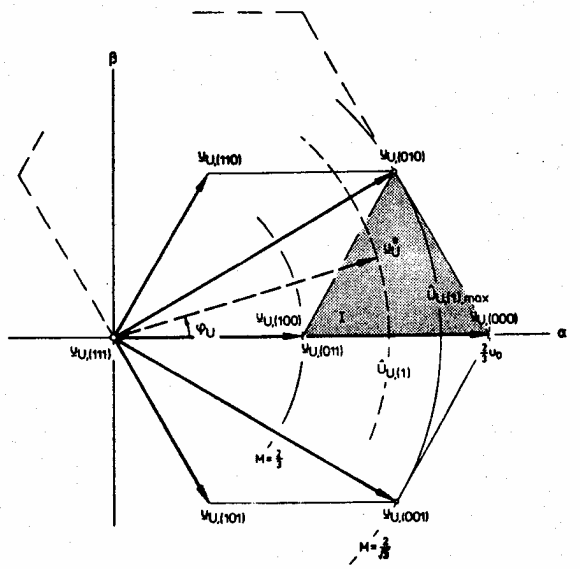

Fig.3: Voltage space vectors $\underline{u}_{U,j}$ associated with the switching states $j = (s_R, s_S, s_T)$ of the PWM rectifier system according to Fig.1(c) for $\varphi_N \in (-\frac{\pi}{6}, +\frac{\pi}{6})$ and/or $i_{N,R} > 0$ and $i_{N,S}, i_{N,T} < 0$.

where

$$M = \frac{\hat{U}_U^*}{\frac{1}{2}U_O} \tag{11}$$

defines the modulation index of the pulse width modulation. The limit towards overmodulation is obtained for

$$M_{\max} = \frac{2}{\sqrt{3}}\,. \tag{12}$$

In this paper we want to treat the system behavior only for typical modulation indices $M \in [\frac{2}{3}, \frac{2}{\sqrt{3}}]$ as they occur for practical realization of PWM rectifier systems.

Under consideration of

$$\delta_{(100)} + \delta_{(000)} + \delta_{(010)} + \delta_{(011)} = 1 \tag{13}$$

also the total relative on-time of the switching states (100) and (011) is given with Eq.(10); it results in

$$\delta_{(100)} + \delta_{(011)} = 1 - \delta_{(000)} - \delta_{(010)} = 2 - \sqrt{3}M\sin(\tfrac{\pi}{3} - \varphi_U)\,. \tag{14}$$

Because both switching states lead to identical voltage space vectors $\underline{u}_{(100)} = \underline{u}_{(011)}$ one can calculate based on a voltage $\underline{u}_U^*$ to be generated basically only the sum $\delta_{(100)} + \delta_{(011)}$, but not a specific distribution of this total on-time among the switching states (100) and (011). The distribution of the redundant voltage vectors between begin and end of each pulse half period constitutes a degree of freedom of the voltage control, therefore. Because, as shown in the following, the distribution has influence on the generation of the current i_M fed into the center point M of the output voltage and also on the mains current ripple, this offers the possibility of an optimization of the system operating behavior (cf. section 3).

2.3 Controllability of the Center Point Current

As is immediately clear based on the structure of the circuit shown in Fig.1(c), turning on $s_i = 1$ of the power transistor of a phase leads to feeding a segment of the respective phase current $i_{N,i}$ into the center point M of the output voltage. Then we have in general

$$i_M = s_R\, i_{N,R} + s_S\, i_{N,S} + s_T\, i_{N,T} \tag{15}$$

for the center point current resulting from the contribution of all phases. Under consideration of Eq.(15) we receive, e.g., for the position of $\underline{u}_U^*$ in the partial triangle I of the space vector plane (cf. Fig.3) and for the switching states j (cf. Eq.(9)) occurring within a pulse period the center point currents compiled in **Tab.1**.

s_R	s_S	s_T	i_M
1	0	0	$+i_{N,R}$
0	0	0	0
0	1	0	$+i_{N,S}$
0	1	1	$-i_{N,R}$

Tab.1: Center point currents i_M of the circuit according to Fig.1(c) in dependency on the switching states (s_R, s_S, s_T).

Because the center point of the output voltage is formed only by capacitive means, special interest is placed now on the local mean value (relatd to a pulse half period)

$$i_{M,\mathrm{avg}} = \frac{1}{\frac{1}{2}T_P}\int_0^{\frac{1}{2}T_P} i_M\{t_\mu\}\,\mathrm{d}t_\mu \tag{16}$$

of the center point current which causes a shift of the voltage center point M. If in a first approximation the ripple of the mains current is neglected and if the mains current is assumed to be approximately constant within $\frac{1}{2}T_P$, there follows for the switching state sequence $(100)-(000)-(010)-(011)$

$$i_{M,\mathrm{avg}} = \delta_{(010)} i_{N,S} + (\delta_{(100)} - \delta_{(011)})\, i_{N,R}\ . \tag{17}$$

As becomes clear by considering the relation $i^*_{N,R} \geq |i^*_{N,S}|$ (which is valid in any case for $\varphi_N \in (-\frac{\pi}{6}, +\frac{\pi}{6})$), the distribution of the total on-time $\delta_{(100)} + \delta_{(011)}$ (which is fixed according to Eq.(14)) between the redundant switching states (100) and (011) has an essential influence on $i_{M,\mathrm{avg}}$. In the following this distribution shall be specified by the ratio

$$\rho_{--} = \frac{\delta_{--}}{\delta_{++} + \delta_{--}} \qquad \rho_{--} \in [0,1]\ . \tag{18}$$

There, δ_{--} denotes in general the relative on-time of the redundant switching state forming a negative center point current contribution; similarily, δ_{++} denotes the relative on-time of the inverse redundant switching state, forming a positive center point current contribution. For the description given here (and being related to Fig.3, sector I) the correspondencies are $\delta_{++} = \delta_{(100)}$ and $\delta_{--} = \delta_{(011)}$. Therefore, then Eq.(17) becomes

$$i_{M,\mathrm{avg}} = \delta_{(010)} i_{N,S} - (1 - 2\rho_{--})(\delta_{(100)} + \delta_{(011)})\, i_{N,R}\ . \tag{19}$$

A symmetric distribution of the redundant switching states between begin and end of each pulse half period is given for $\rho_{--} = 0.5$.

The controllability of $i_{M,\mathrm{avg}}$ by the parameter ρ_{--} is (as described, e.g., in [11]) in general applied for the control of the symmetry of the output partial voltages. If an unsymmetric distribution of the output voltage is given, a transient mean value $i_{M,\mathrm{avg}}$ of the center point current i_M is generated by appropriate variation of ρ_{--}, correcting the unsymmetry. As a result, $I_{M,\mathrm{avg}} = 0$ is guaranteed in the average over a fundamental period thereby ($I_{M,\mathrm{avg}}$ denotes the global mean value of i_M, related to the fundamental). For the further considerations (cf. section 3.1) we have to point out here, however, that by the requirement $I_{M,\mathrm{avg}} = 0$ the shape $\rho_{--} = \rho_{--}\{\varphi_U\}$ is not defined unequivocally. This offers the possibility to optimize the operating behavior of the system.

Remark: According to Eq.(17) $i_{M,\mathrm{avg}}$ is formed in general by a component which can be influenced by ρ_{--} and by a component which is directly given by the voltage $\underline{u}^*_U$ to be generated an by a phase current. As an analysis of an entire mains period shows the current component which cannot be influenced shows ideally a periodic shape with 3 times the mains frequency and with no DC component. Therefore, also for $\rho_{--} = 0.5$ (and/or $\delta_{(100)} - \delta_{(011)} = 0$ in the region I of Fig.3 or in general $\delta_{++} = \delta_{--}$) ideally no shift of the center point potential results within a fundamental period in the stationary case.

2.4 Harmonics of the Mains Current with Switching Frequency

The current consumption $\underline{i}_N$ of the rectifier system in general is determined by the difference of the mains voltage $\underline{u}_N$ and the rectifier input voltage $\underline{u}_{U,j}$

$$L\frac{\mathrm{d}\underline{i}_N}{\mathrm{d}t} = \underline{u}_N - \underline{u}_{U,j}\ . \tag{20}$$

In conncetion with Eq.(4) there results, therefore, the relation

$$\Delta\underline{i}_N = \underline{i}_N - \underline{i}^*_N \tag{21}$$

for the deviation of the actual mains current shape $\underline{i}_N$ from the ideal purely sinusoidal shape $\underline{i}^*_N$

$$L\frac{\mathrm{d}\Delta\underline{i}_N}{\mathrm{d}t} = \underline{u}^*_U - \underline{u}_{U,j}\ . \tag{22}$$

As Eq.(22) shows clearly, the mains current harmonics with switching frequency are caused by the difference between the space vector $\underline{u}^*_U$ (which has to be formed for a purely sinusoidal current shape) and the space vector $\underline{u}_{U,j}$ which is actually present. By a change of the time-weighting and/or the distribution ρ_{--} of the redundant switching states besides i_M also the trajectory of the space vector $\Delta\underline{i}_N$ is influenced, therefore. Equally, the time shape of the ripple component of the mains phase currents is influenced.

However, one has to point out there that the voltage space vector $\underline{u}_{U,\mathrm{avg}}$ according to Eq.(8) (which results in the average over a pulse half period) is not influenced by a variation in ρ_{--}. If we have $\underline{u}_{U,\mathrm{avg}} = \underline{u}^*_U$ then based on

$$\Delta\underline{i}_{N,t_\mu=0} = 0 \tag{23}$$

after moving through the triangular trajectory with the corner points

$$\begin{aligned}
\Delta\underline{i}_{N,t_{\mu,1}} &= \delta_{(100)}(\underline{u}^*_U - \underline{u}_{U,(100)})\frac{T_P}{2L}\\
\Delta\underline{i}_{N,t_{\mu,2}} &= \Delta\underline{i}_{N,t_{\mu,1}} + \delta_{(000)}(\underline{u}^*_U - \underline{u}_{U,(000)})\frac{T_P}{2L}\\
\Delta\underline{i}_{N,t_{\mu,3}} &= \Delta\underline{i}_{N,t_{\mu,2}} + \delta_{(010)}(\underline{u}^*_U - \underline{u}_{U,(010)})\frac{T_P}{2L}\ .
\end{aligned} \tag{24}$$

linked to the time values $t_{\mu,1}$, $t_{\mu,2}$ and $t_{\mu,3}$, with high accuracy

$$\Delta\underline{i}_{N,t_\mu=\frac{1}{2}T_P} = 0 \tag{25}$$

is fulfilled at the end of each pulse half period for high pulse frequency. For further consideration of the reversal of the switching state sequence after each pulse half period (cf. Eq.(9)) then in the average over a pulse period always a sinusoidal control of the phase currents is given. For a variation of ρ_{--} during an optimization the side condition of a sinusoidal mains current shape is implicitely met already, therefore, and has not to be considered further.

3 Optimal Control of the System, Optimization Criteria

As the previous considerations show, the control parameter ρ_{--} influences the generation of the ripple $\Delta\underline{i}_N$ of the mains phase currents as well as the generation of the center point current i_M. Therefore, it is obvious to consider possibilities of an optimization of the system behavior by properly given ρ_{--}.

In the literature in most cases the goal of an optimization of the operating behavior of high-frequency PWM three-level converter systems is defined by minimizing the low-frequency variation of the potential u_M of the output voltage center point [12]–[14], [10] (and/or the possibility for applying of ρ_{--} for the control of u_M is treated in general [15], [8], [11]). The influence of this optimization on the AC-side operating behavior is not analyzed in greater detail there. Therefore, in the following (after a short discussion of different optimization criteria) we want to calculate and critically compare by digital simulation the operating behavior on the AC-side for an optimization on the DC-side and, vice versa, the operating behavior on the DC-side for an optimization on the AC-side.

3.1 Optimization of the Operating Behavior on the DC-Side

3.1.1 Minimization of the Local Average Value of the Center Point Current

According to Eq.(19), one can influence the local average value $i_{M,\mathrm{avg}}$ of the center point current i_M by the parameter ρ_{--}. If a local average value $i_{M,\mathrm{avg}}$ results, the potential u_M of M is shifted in the average over a pulse period according to

$$\frac{\mathrm{d}}{\mathrm{d}t}u_{M,\mathrm{avg}} = \frac{1}{2C} i_{M,\mathrm{avg}}\ . \tag{26}$$

This leads to an unsymmetric distribution of the output voltage, resulting in an increase of the blocking voltage stress on the power semiconductors of a bridge half and in the occurrence of low-frequency even numbered harmonics of the phase voltages $u_{U,i}$ (cf. Fig.3 in [15]). If the asymmetry of the voltage distribution for minimum capacitance C of the output capacitors (and/or for high power density of the converter) shall be limited to a minimum value one has to strive for

$$i_{M,\mathrm{avg}} \to 0 \tag{27}$$

by appropriately given ρ_{--} for each pulse interval, therefore. If, e.g., by appropriately high dynamics of the center point voltage control $i_{M,\mathrm{avg}} = 0$ is fulfilled ideally then i_M has only spectral components with switching frequency but not such with low frequency. For sufficiently high pulse frequency this makes possible the suppression of stationary oscillations of the center point potential by foil capacitors instead of electrolytic capacitors (with comparatively higher specific capacitance, but shorter life time).

The value ρ_{--} which leads to $i_{M,\mathrm{avg}} = 0$ can be calculated directly based on the relation $i_{M,\mathrm{avg}} = i_{M,\mathrm{avg}}\{\rho_{--}\}$ being valid in the respective region of the space vector plane. There follows, e.g., for the region I (pointed out in Fig.3 by the dotted area) under consideration of Eqs.(10), (14) and (19) and under the assumption of approximate phase equality $\varphi_U \approx \varphi_N$ of $\underline{u}^*_U$ and $\underline{u}_N$ and/or $\underline{i}^*_N \approx \underline{i}_N$ (cf. Gl.(4))

$$\rho_{--,I}|_{i_{M,\mathrm{avg}}=0} = \frac{1}{2}\Big[1 + \frac{\sin(\varphi_U)\cos(\varphi_U)}{\cos(\varphi_U - \frac{2\pi}{3})(\frac{2}{\sqrt{3}M} - \sin(\varphi_U + \frac{\pi}{3}))}\Big]\ . \tag{28}$$

For $\rho_{--} = \rho_{--,I}|_{i_{M,\mathrm{avg}}=0}$ the negative contribution $\delta_{(010)} i_{N,S}$ ($i_{N,S} < 0$) to $i_{M,\mathrm{avg}}$ (as caused by the switching state (010)) is compensated exactly by the positive contribution $(1 - 2\rho_{--})(\delta_{(100)} + \delta_{(011)}) i_{N,R}$ ($i_{N,R} > 0, \rho_{--} < 0.5$) of the redundant switching states. Because the switching state (010) gets higher weight with rising M but the relative on-time of the redundant

switching states is reduced with increasing modulation index (cf. Eqs.(10) and Eq.(14)), $i_{M,\mathrm{avg}} = 0$ can be guaranteed only for modulation indices

$$M \le M_{\mathrm{lim}} = \min\{\frac{2}{\sqrt{3}}(\sin(\varphi_U + \frac{\pi}{3}) - \tan(\varphi_U)\cos(\varphi_U - \frac{2\pi}{3}))^{-1}\} \approx 1.1 \,, \tag{29}$$

however. In the case considered here, ρ_{--} becomes 0 for $M = M_{\mathrm{lim}}$ (and/or ρ_{++} becomes 1). The time-weighting of the redundant switching states cannot be shifted further, therefore. For $M > M_{\mathrm{lim}}$ $\rho_{--} = 0$ is maintained; exclusively $\underline{u}_{U,(100)}$ is applied for forming the voltage. Therefore, low-frequency spectral components of i_M result. However, due to the symmetries of three-phase systems $I_{M,\mathrm{avg}} = 0$ is guaranteed in any case. (Here, it is assumed that unsymmetries caused, e.g., by differences in the capacitance of the output capapcitors or not equal switching times of the valves, can be neglected; cf. section 5 in [25]).

Concerning $M_{\mathrm{lim}} \approx 1.1$ we want to note that this value corresponds to an output voltage $U_O \approx 590\,\mathrm{V}$ for an input phase voltage of $U_{N,\mathrm{rms}} = 230\,\mathrm{V}$ ($\approx U_{U,\mathrm{rms}}$). Because PWM rectifier systems which are operated in the European low voltage mains have typically DC link voltages in the region $U_O = 620 \ldots 750\,V$ (and which therefore can be operated with modulation indices $M < 1.05$ in the stationary case) usually the possibility of controlling the rectifier system with $i_{M,\mathrm{avg}} = 0$ is given.

3.1.2 Minimization of the Local RMS Value of the Output Capacitor Current

If the output capacitors C are realized by electrolytic capacitors, the optimization goal will be set advantageously as minimization of the rms value of the output capacitor current

$$I_{C,\mathrm{rms}} \to \mathrm{Min} \tag{30}$$

rather than Eq.(27). This is the case because the electrolytic capacitors typically have a life-time which heavily depends on the current stress (and/or the core temperature). The capacitance value (or physical size of the capacitor) to be provided therefore is often determined by the power loss $I^2_{C,\mathrm{rms}} R_{\mathrm{ESR}}$ (ESR denotes the equivalent series resisitance of the capacitor) to be dissipated and not by a given admissible variation of the center point potential.

If the minimization of the rms current stress on the output capacitors due to a change of the distribution ρ_{--} is analyzed in more detail, e.g., by analytic calculations and digital simulation [16], one can see, however, that independently of ρ_{--} always

$$I_{C,\mathrm{rms}} = \frac{10\sqrt{3}M}{8\pi} - \frac{9M^2}{16} \tag{31}$$

results. As can be checked by the analytical proof as given in the following, $I_{C,\mathrm{rms}}$ is not available for optimization, therefore!

For the calculation of the rms value of the capacitor current one assumes according to

$$I^2_{C,\mathrm{rms}} = \frac{1}{2}(I^2_{C+,\mathrm{rms}} + I^2_{C-,\mathrm{rms}}) \tag{32}$$

an equal current stress on both output capacitors C_+ and C_-; this can be done due to the symmetric structure of the power circuit and due to the phase-symmetric control of the system. The load current i_O is assumed to be constant ($i_O = I_O$). The global rms value according to Eq.(32) can now be calculated by global averaging of the local rms values and/or rated power loss contributions $i^2_{C+,\mathrm{rms}}$ and $i^2_{C-,\mathrm{rms}}$ of the single pulse intervals

$$I^2_{C,\mathrm{rms}} = \frac{1}{T_N}\int_{T_N} \frac{1}{2}(i^2_{C+,\mathrm{rms}} + i^2_{C-,\mathrm{rms}})\,\mathrm{d}t \tag{33}$$

(T_N denotes the mains period). With

$$i^2_{C\pm,\mathrm{rms}} = \frac{1}{\frac{T_P}{2}}\int_{\frac{T_P}{2}} i^2_{C\pm}\{t_\mu\}\,\mathrm{d}t_\mu \tag{34}$$

and

$$i_{C+} = i_+ - I_O \qquad i_{C-} = i_- + I_O \tag{35}$$

(cf. Fig.1(c)) there follows under consideration of

$$\frac{1}{T_N}\int_{T_N} i_+\,\mathrm{d}t = \frac{1}{T_N}\int_{T_N} i_-\,\mathrm{d}t = I_O \,, \tag{36}$$

$$I^2_{C,\mathrm{rms}} = \frac{1}{T_N}\int_{T_N}[\tfrac{1}{T_P}\textstyle\int_{\frac{T_P}{2}}(i^2_+ + i^2_-)\,\mathrm{d}t_\mu]\,\mathrm{d}t \;-\; I^2_O. \tag{37}$$

As, e.g., the analysis of the current values i_+ and i_- resulting in region I (cf. Fig.3) of the space vector plane (switching state sequence (100)-(000)-(010)-(011)) shows during the on-time of the redundant switching states (100) or (011) always one of the currents i_+ or i_- becomes 0 (cf. **Tab.2**); the currents being not zero therefore have the same value and the same sign ($i_{-,(100)} = i_{+,(011)} = i_R$). For the local averaging in Eq.(37) we have, therefore, in region I

$$\frac{1}{T_P}\int_{\frac{T_P}{2}}(i^2_+ + i^2_-)\mathrm{d}t_\mu = \frac{1}{2}[i^2_R(\delta_{(100)} + \delta_{(011)}) + 2i^2_R\delta_{(000)} + (i^2_R + i^2_T)\delta_{(010)}] \,. \tag{38}$$

There, only the sum of the relative on-times of the redundant switching states (100) and (011) appears. Therfore, also a distribution ρ_{--} varying arbitrarily with time but meeting the assumed phase symmetry has no influence on $I_{C,\mathrm{rms}}$. The capacitor current stress therefore is defined only by the amplitude of the fundamental $\hat{I}_{N,(1)}$ of the mains current and by the modulation index M if variations with switching frequency are neglected).

s_R	s_S	s_T	i_+	i_-
1	0	0	0	i_R
0	0	0	i_R	i_R
0	1	0	i_R	$-i_T$
0	1	1	i_R	0

Tab.2: Currents i_+ and i_- in the positive and negative output voltage bus in dependency on the switching state (s_R, s_S, s_T).

3.2 Optimization of the Operating Behavior on the AC-Side

For the optimization of the AC-side operating behavior of PWM inverter and PWM rectifier systems with high switching frequency frequently the square of the global rms value of the phase current ripple

$$\Delta I^2_{N,\mathrm{rms}} \to \mathrm{Min} \tag{39}$$

is used as optimization criterion [17]-[19]. Eq.(39) represents in general a quadratic optimization criterion which corresponds in a physically clear manner to the minimization of the AC-side harmonic losses of the rectifier system if the frequency dependency of the resistance of the series inductances and of the resistive component of the mains source impedance is neglected.

For the calculation and/or minimization of $\Delta I_{N,\mathrm{rms}}$ one can apply advantageously the respresentation of the time behavior of the ripple components $\Delta i_{N,i}$ of the phase currents $i_{N,i}$ as trajectory of the associated space vector $\Delta\underline{i}_N$. (The dependency of the trajectory of the space vector $\Delta\underline{i}_N$ and/or the phase quantities $\Delta i_{N,i}$ gained from it by projection on the phase axes of ρ_{--} already have been pointed out in section 2.4.) With

$$\Delta i^2_{N,R} + \Delta i^2_{N,S} + \Delta i^2_{N,T} = \frac{3}{2}|\Delta\underline{i}_N|^2 \tag{40}$$

(cf. Eq.(14) in [20]) one can calculate the rated local harmonic power loss of the system within a pulse half period via

$$\Delta i^2_{N,RST,\mathrm{rms}} = \frac{3}{T_P}\int_{t_\mu=0}^{t_\mu=\frac{1}{2}T_P} |\Delta\underline{i}_N|^2\,\mathrm{d}t_\mu \,. \tag{41}$$

There, $i_{N,RST,\mathrm{rms}}$ has to be interpreted as a local rms value of the mains current harmonics describing the total effect of the phases. Under consideration of the symmetries of a three-phase system one can now determine the rated global harmonic power loss of one phase by a summation of the contributions of the single pulse half periods. If the summation is replaced for a switching frequency being high as compared to the mains frequency by an integration, we have

$$\Delta I^2_{N,\mathrm{rms}} = \frac{1}{2\pi}\int_0^{\frac{2\pi}{3}} \Delta i^2_{N,RST,\mathrm{rms}}\,\mathrm{d}\varphi_U \,. \tag{42}$$

Because for the calculation of $I^2_{N,\mathrm{rms}}$ according to Eq.(42) one integrates always over positive contributions $\Delta i^2_{N,RST,\mathrm{rms}}$ of the single pulse periods one can also replace the global optimization criterion according to Eq.(39) by a minimization of the local contributions

$$\Delta i^2_{N,RST,\mathrm{rms}} \to \mathrm{Min} \,. \tag{43}$$

As is immediately clear by inspection one has to form (for $\Delta i^2_{N,RST,\mathrm{rms}} \to$ Min) the trajectory being followed by $\Delta\underline{i}_N$ within each pulse half period by proper setting of ρ_{--} such that a minimum average distance from the origin results (cf. Gl.(41)).

Remark: In the literature one discusses in connection with the optimization of three-level converter systems besides the minimization of the harmonic losses $\Delta I^2_{N,\mathrm{rms}}$ also, e.g., the elimination of (low frequency) spectral components of the mains current (selected harmonic elimination [18]) or a minimization of the peak values of the phase currents (cf. p. 3.77 in [21]). Due to the assumed high switching frequency these optimizations (in most cases related to systems of high power and, therefore, with low switching frequency) cannot be performed in a sensible manner due to the high computational effort; also, such optimizations are not required for high switching frequency. The optimization of the AC-side operating behavior is limited to $\Delta I^2_{N,\mathrm{rms}}$, therefore.

3.3 Minimization of the Stress on the Power Semiconductors

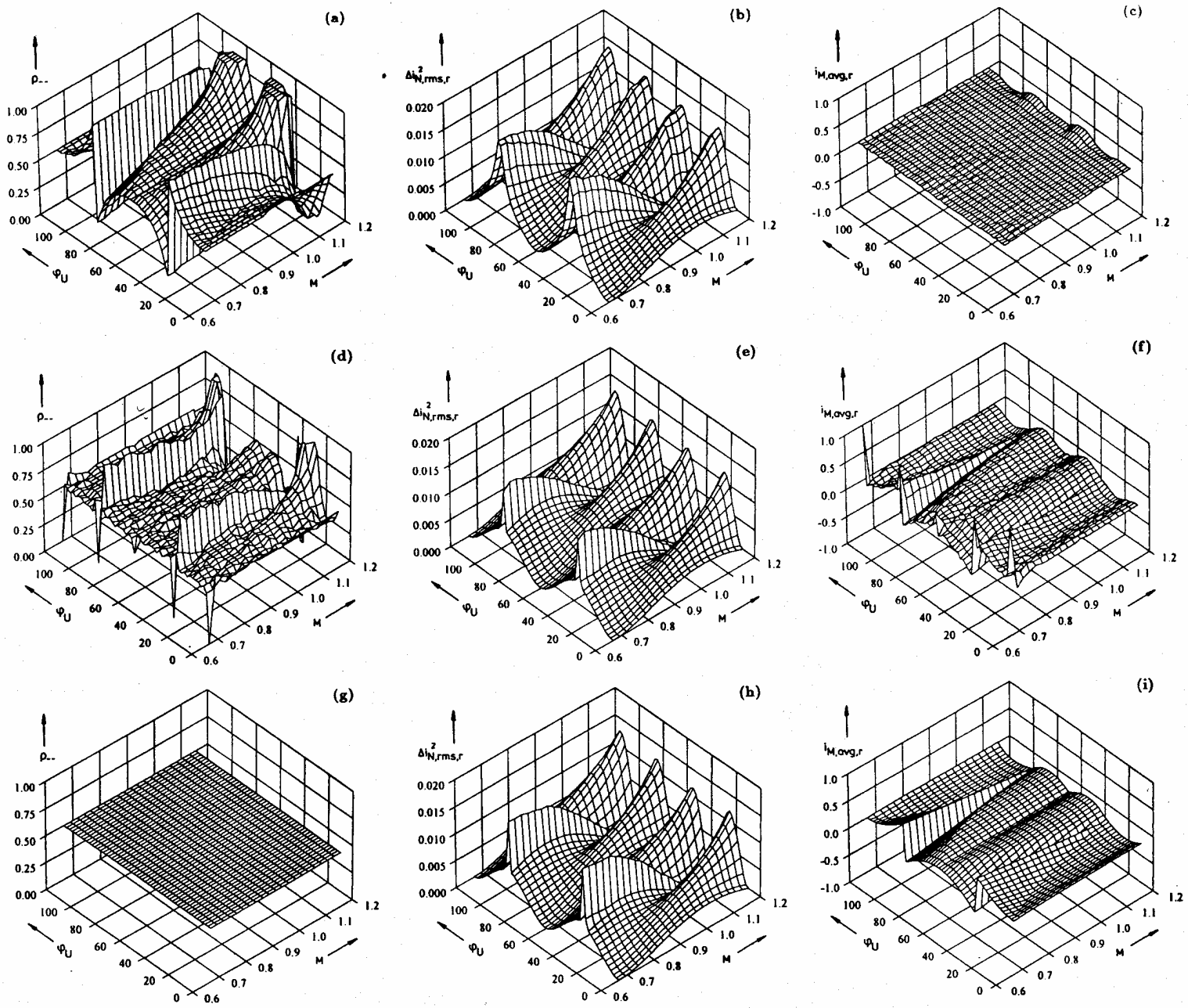

Fig.4: Distribution ρ_{--} of the redundant switching states and local optimization criteria $\Delta i^2_{N,\mathrm{rms}}$ (the contribution of $\Delta i^2_{N,RST,\mathrm{rms}}$ being related to one phase) and $i_{M,\mathrm{avg}}$ for minimization of the absolute value of the local mean value $i_{M,\mathrm{avg}}$ of the center point current i_M (cf. **(a)**, **(b)** and **(c)**), for minimization of the local harmonic losses $\Delta i^2_{N,\mathrm{rms}}$ of the mains current (cf. **(d)**, **(e)** and **(f)**) for suboptimal selection $\rho_{--} = 0.5$ of the optimization parameter ρ_{--} (cf. **(g)**, **(h)** and **(i)**). As is checked by (c) in consistency with Eq.(29), $i_{M,\mathrm{avg}} = 0$ can only be obtained for $M <\approx 1.1$.

Based on the possibilities discussed here concerning a minimization of the harmonic load on the mains or of the stress on the output capacitors finally the question is asked whether via a proper selection of ρ_{--} also a minimization of the stress on the power semiconductors (average value or rms value of the current or low switching losses) can be achieved.

As an analysis shows (which is not described here in more detail for the sake of brevity) the fundamental-related current stress of the circuit elements are only influenced to a minor extent by a change or time-dependent variation of ρ_{--} (similary to the rms value of the output capacitor current). The on-state losses of the system cannot, therefore, be reduced via ρ_{--}. However, by proper choice of $\rho_{--} = 0$ or 1 within defined intervals of the mains period one can suppress the occurrence of switching losses of one bridge leg at a time. This becomes clear by considering of the switching state sequence resulting for $\rho_{--} = 1$ or $\delta_{(100)} = 0$ in the region I of the space vector plane (cf. Fig.3)

$$\ldots|_{t_s=0}(\underline{0}00)-(\underline{0}10)-(\underline{0}11)|_{t_s=\frac{1}{2}T_P}(\underline{0}11)-(\underline{0}10)-(\underline{0}00)|_{t_s=T_P}\cdots . \quad (44)$$

For appropriate control of the phases S and T each phase is not being switched in the vicinity of the maximum of the associated mains current. Therefore, a significant reduction of the switching losses of the system is obtained. According to Eq.(19) there occurs a relatively high stress on the center point M by low frequency current harmonics, however, because for $\rho_{--} = 1$ or 0 certainly no mutual compensation of the center point current components of the single switching states within a pulse half period is given (cf. Eq.(28)). The discontinuous modulation of three-level converters therefore shall not be treated here, but shall be analyzed in more detail in a future paper.

3.4 Digital Simulation, Normalizations

The calculation of the optimum distribution $\rho_{--} = \rho_{--}\{M, \varphi_U\}$ of the redundant switching states can only be performed analytically for $i_{M,\mathrm{avg}} \rightarrow 0$ (cf. Eq.(28)). For the minimization of the harmonic losses $\Delta I^2_{N,\mathrm{rms}} \rightarrow \mathrm{Min}$ an analytical calculation leads to relatively complex expressions. Therefore, the system behavior is analyzed by digital simulation in this case. Due to the symmetries of three-phase systems the considerations could be limited to $\frac{1}{6}$ of the mains period. In order to give a clear representation and simple check of the observance of the symmetry conditions, the calculation and optimization is extended to $\frac{1}{3}$ of the fundamental period, however (cf. Fig.4).

For the simulation parameters we select those rated quantities which are characteristic for an application of the system with the European low voltage mains (e.g., for application as input stage of an uninterruptible power supply, cf. section 3 in [22])

$$\begin{array}{lcl} U_{N,\mathrm{rms}} & = & 230\,\mathrm{V} \\ U_O & = & 700\,\mathrm{V} \\ \hat{I}^*_N & = & 18\,\mathrm{A} \\ f_P & = & 16\,\mathrm{kHz} \\ L & = & 1\,\mathrm{mH}\,. \end{array}$$

The relatively low value of the converter switching frequency $f_P = 16\,\mathrm{kHz}$ is set with respect to a short simulation time. A change of the modulation index (rated value $M = 0.93$) is obtained for constant output voltage U_O via changing the mains voltage amplitude $\hat{U}_N$. In order to point out the essential features we assume U_O to be impressed. This makes possible to avoid the design and simulation of the output voltage control loop. The guidance of the mains currents is realized by setting the space vector $\underline{u}^*_U$ (cf. Eq.(8)) which is present in the average over a pulse period in such a way that the mains current space vector $\underline{i}_N$ is transferred from one point of the reference value circle $\underline{i}^*_N$ into a position which has a time difference of $\frac{1}{2}T_P$. One also can say that it is moved (seen as time average) along the reference value circle. This circle is defined by the phase current fundamental. By application of this predictive current control method according to the deadbeat principle we can avoid the calculation of an initial transient oscillation of the current control. Therefore, we can simulate the stationary operating behavior directly.

3.4.1 Normalization

In order to obtain most general conclusions (which are not limnited to specific operating parameters and device characteristics) by the simulation, the calculated rms value of the mains current harmonics $\Delta I_{N,\mathrm{rms}}$ is given in normalized form by

$$\Delta I_{N,\mathrm{rms,r}} = \frac{1}{\Delta I_\mathrm{r}} \Delta I_{N,\mathrm{rms}} \quad (45)$$

with

$$\Delta I_\mathrm{r} = \frac{U_O T_P}{8L}\,. \quad (46)$$

$\Delta I_{N,\mathrm{rms,r}}$ represents a characteristic value being independent of $f_P = T_P^{-1}$

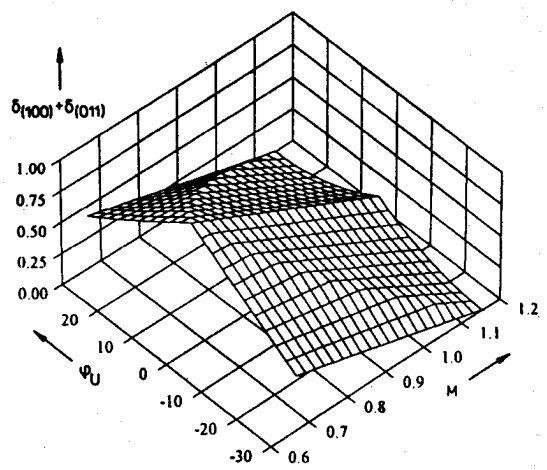

Fig.5: Sum $\delta_{(100)}+\delta_{(011)}$ of the relative on-times of the redundant switching states (100) and (011) in dependency on the modulation index M and on the position $\varphi_U \in (-\frac{\pi}{6}, +\frac{\pi}{6})$ of a pulse interval.

and L in a first approximation . For the time-dependency of $i_{M,\mathrm{avg}}$ and for the amplitudes $\hat{I}_{M,(k)}$ of the low-frequency harmonics of the center point current we have according to

$$i_{M,\mathrm{avg,r}} = \frac{1}{\hat{I}_{N,(1)}} i_{M,\mathrm{avg}} \quad (47)$$

the amplitude of the mains current fundamental $\hat{I}_{N,(1)} = \hat{I}^*_N$ as normalization basis. This eliminates the direct dependency of i_M on $\hat{I}_{N,(1)}$.

4 Comparison of the Optimal Control Methods

4.1 Results of the Local Optimization

In order to make possible a direct comparison of the local system behavior for $i_{M,\mathrm{avg}} \rightarrow 0$ and $\Delta i^2_{N,RST,\mathrm{rms}} \rightarrow \mathrm{Min}$, we have shown in **Fig.4** (a) - (f) the dependencies of ρ_{--}, $\Delta i^2_{N,\mathrm{rms}} = \frac{1}{3}\Delta i^2_{N,RST,\mathrm{rms}}$ and $i_{M,\mathrm{avg}}$ on the modulation index M and the position φ_U of a pulse interval within the mains period resulting for each case.

Concerning the distribution ρ_{--} relatively much different conditions exist for DC-side and AC-side optimization, especially for high modulation index. This effects $i_{M,\mathrm{avg}}$ and $\Delta i^2_{N,\mathrm{rms}}$ in an only much reduced manner, however. The low influence of ρ_{--} can be explained by the fact that (as **Fig.5** shows and as can be seen from Eq.(14)) the overall on-time of the redundant switching states is decreased with rising M; at the control limit $M = \frac{2}{\sqrt{3}}$ it has values close to 0. The operating behavior of the system therefore is influenced only to a minor extent by the distribution of the on-time (compare Figs.4(b) and (e) and Figs.4(c) and (f)).

Based on Fig.4(d) one can give with $\rho_{--} = 0.5$ a very good and simple realizable approximation of a harmonic-optimum control method (compare Figs.4(e) and (h) [33]). It is interesting to note that $\rho_{--} = 0.5$ represents a suboptimal control method also for two-level converters. Also there the distribution of the redundant switching states (of the two free-wheeling states) between begin and end of each pulse half period results in an approximately harmonic-optimal control (cf. Fig.6 in [20]).

Remark: In Figs.4(d) and (e) for $\varphi_U = \frac{\pi}{6}$ a discontinuity of the shape of ρ_{--} and $\Delta i^2_{N,\mathrm{rms}}$ in dependency on φ_U is apparent. The reason for this discontinuity is the discontinuity of the phase currents of unidirectional three-level PWM rectifier systems at the zero crossings and/or the voltage generation of these systems which is linked to the direction of the phase current flow (as mentioned in section 2.1). Because the effect remains limited to one pulse period, the global operating behavior (being of main interest) is only changed to a minor extent by this, as compared to bidirectional systems. Therefore, one can omit a more detailed discussion.

4.2 Global Harmonic Losses and Spectrum of the Center Point Current

The integration of the local harmonic losses $\Delta i^2_{N,\mathrm{rms}}$ shown in Figs.4(b), (e) and (h) lead to the relation of the global harmonic losses $\Delta I^2_{N,\mathrm{rms}}$ in dependency on M as shown in **Fig.6**. Furthermore, **Fig.7** shows the

amplitudes $\hat{I}_{M,(k)}$ of the low-frequency harmonics of i_M in normalized form as they are of interest for the determination of the capacitance of the output capacitors (k denotes the ordinal number of the current and voltage harmonics related to the mains frequency).

The amplitudes $\hat{I}_{M,(k)}$ are obtained for given M via a Fourier analysis of the shapes $i_{M,\mathrm{avg}} = i_{M,\mathrm{avg}}\{\varphi_U\}$ as given in Figs.4(c), (f) and (i). For the dimensioning of the output capacitors we have to guarantee

$$C \geq \frac{1}{k\,\omega_N\,\hat{U}_{C,(k)}}\,\hat{I}_{C,(k)}\,. \tag{48}$$

in order to not exceed a given amplitude $\hat{U}_{C,(k)}$ of the voltage variation due to $\hat{I}_{C,(k)}$ For constant output voltage (highly dynamic output voltage control) a parallel connection of the output capacitors is in effect for i_M (cf. section 5.2 in [16]); therefore, for the harmonics of the capacitor current we have

$$\hat{I}_{C,(k)} = \frac{1}{2}\hat{I}_{M,(k)}\,. \tag{49}$$

According to Eq.(48) the lowest order harmonic ($k = 3$) has the maximum influence on the determination of the capacitance.

With Fig.6 and Fig.7 we now have the possibility of direct assessment and/or comparison of the DC- and AC-side operating behavior of an only DC-side or an only AC-side optimal control and of a suboptimal control of a three-level PWM rectifier system.

Concerning the mains-side harmonic losses $\Delta I^2_{N,RST,\mathrm{rms}}$ all control methods show only relatively small differences. The selection of ρ_{--} has a larger influence on the amplitude of the 3rd harmonic of i_M. This amplitude is limited to very small values only for the optimization $i_{M,\mathrm{avg}} \to 0$. We want to point out as most important result, therefore, that for an advantageous dimensioning of the system on the AC- and DC-sides we have to apply as basis for a control method the distribution $\rho_{--} = \rho_{--}\{M, \varphi_U\}$ resulting for $i_{M,\mathrm{avg}} \to 0$.

5 Optimum Modulation Functions

The determination of the switching times of the bridge legs of the rectifier system can basically be carried out based on a voltage space vector $\underline{u}^*_U$ or by intersecting the phase modulation functions m_i with a positive and a negative triangular carrier signal (subharmonic oscillation method, cf. Fig. 4 in [24]). For the subharmonic oscillation method we have to convert ρ_{--} into a zero voltage component m_0 which generalizes a triple of purely sinusoidally shaped phase modulation functions m'_i.

According to Eq.(11) we have for the time-dependency of the phase modulation functions in general

$$m_i = \frac{1}{\frac{1}{2}U_O}\,u_{U,i,\mathrm{avg}} = m'_i + m_0\,. \tag{50}$$

The local mean value $u_{U,i,\mathrm{avg}}$ of the rectifier input phase voltages $u_{U,i}$ has to be calculated there based on Eq.(1) and on the respective given relative on-times of the switching states. E.g., there follows for the region I of the space vector plane (cf. Fig.3 and Eq.(9))

$$\begin{aligned} m_{R,I} &= \delta_{(000)} + \delta_{(010)} + \delta(011) \\ m_{S,I} &= -\delta_{(100)} - \delta_{(000)} \\ m_{T,I} &= -\delta_{(100)} - \delta_{(000)}) - \delta(010) \end{aligned} \tag{51}$$

and

$$\begin{aligned} m'_{R,I} &= \frac{2}{3}(1 + \delta_{(000)} + \frac{1}{2}\delta_{(010)}) \\ m'_{S,I} &= -\frac{1}{3}(1 + \delta_{(000)} - \delta_{(010)}) \\ m'_{T,I} &= -\frac{1}{3}(1 + \delta_{(000)} + 2\delta_{(010)}) \end{aligned} \tag{52}$$

and for the zero-quantity m_0 being equal for all phases

$$m_{0,I} = \frac{1}{3}(m_R + m_S + m_T) = -\frac{1}{3}\delta_{(000)} + (\rho_{--} - \frac{2}{3})\,(\delta_{(100)} + \delta_{(011)}) \tag{53}$$

As Eqs.(52) and (53) prove clearly, a change of ρ_{--} influences only the zero-quantity m_0; the zero-quantity-free components m'_i of the modulation functions (which guarantees the mains-frequency sinusoidal shape of the phase currents in connection with the mains voltage) remain unchanged. The modulation functions (as allocated to the different optimizations) therefore are distinguished only regarding their zero-quantity component m_0.

As an example Fig.8 shows the shape of m_R and m_0 ($M = 0.93$) as given for the different control methods within a mains period. It is important to point out that (as Fig.8(a) clearly shows and as is confirmed by a calculation check) the shape of m_0 can be approximated for $i_{M,\mathrm{avg}} \to 0$ with sufficient accuracy by a 3rd harmonic $m_{(3)}$. This harmonic shows (in the control region $M \in [\frac{2}{3}, \frac{2}{\sqrt{3}}]$ treated here) an amplitude which is directly linked to the amplitude $M_{(1)} = M$ of the fundamental m'_i of m_i

$$M_{(3),i_{M,\mathrm{avg}}\to 0} \approx \frac{1}{4}M_{(1)}\,. \tag{54}$$

Therefore, especially for digital realization of the control a very simple relizability is given.

Remark: Also concerning the amplitude of the 3rd harmonic an interesting relationship between two-level and three-level power converter systems is given. As shown in [26], $M_{(3)} \approx \frac{1}{4}M_{(1)}$ gives also for two-level converters an optimal solution concerning the voltage ripple (which has switching frequency there, however) of the output capacitor. Concerning the AC-side current harmonics this represents a suboptimal solution.

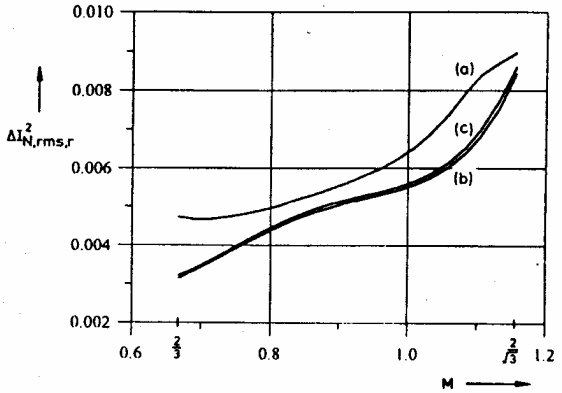

Fig.6: Related global harmonic losses $\Delta I^2_{N,\mathrm{rms},r}$ of one phase of a three-level PWM rectifier system (cf. Eq.(42)) for minimum loading of the output voltage center point by low-frequency harmonics $i_{M,\mathrm{avg}} \to 0$ (cf. (a)), harmonic-optimal control $\Delta i^2_{N,\mathrm{rms}} \to \mathrm{Min}$ (cf. (b)), and suboptimal modulation $\rho_{--} = 0.5$ (cf. (c)).

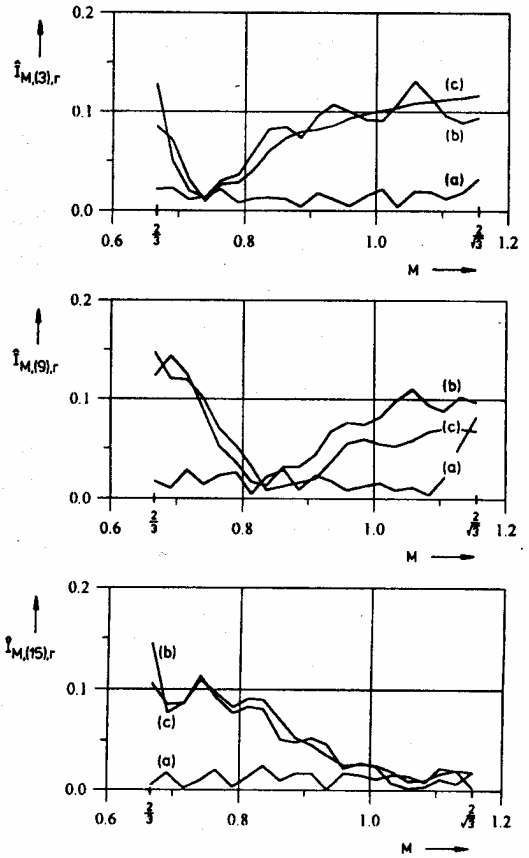

Fig.7: Low-frequency harmonics $\hat{I}_{M,(k)}$, $k = 3, 9, 15$ of the center point current i_M in dependency on the modulation index M for (a), (b), and (c) according to Fig.6. The limit $M_{\mathrm{lim}} \approx 1.1$ of the realizability of $i_{M,\mathrm{avg}} = 0$ (as mentioned in connection with Fig.4) becomes clear also by the shape of $\hat{I}_{N,(9)} = \hat{I}_{N,(9)}\{M\}$ for control method (b).

6 Control of the Potential of the Output Voltage Center Point

By the different optimizations the distribution ρ_{--} within each pulse interval is defined. Therefore, no degree of freedom for control of the potential u_M of the output voltage center point M remains in order to equalize possible unsymmetries of the system. In any case, a requirement for a practical realization of the control methods is, therefore, that for each control method described previously there does not occur a mean value $I_{M,\mathrm{avg}}$ of i_M for ideal system function:

$$I_{M,\mathrm{avg}} = 0 \,. \tag{55}$$

As Figs.4(c), (f) and (i) clearly show (and as can be checked by digital simulation), Eq.(55) is fulfilled by the AC-side optimum as well as by the DC-side optimum and by the suboptimum control method. Despite this, for the stationary equalization of the unsymmetries which always occur in real systems (e.g., differences in the capacitances of the positive and negative DC-link capacitors) we have to provide a control of the center point potential. This control gives by a small change of the optimum distribution ρ_{--} a symmetrization of the output partial voltages.

The control of the center point potential has to be realized appropriately for the respective voltage control method. For harmonic optimum control we have to limit the dynamics of the center point voltage control loop to such an extent that the local distribution ρ_{--} (being required for the minimization of the harmonic losses) is not influenced. The control of u_M then is performed in the average over a mains period by an offset of ρ_{--} as given by the center point voltage controller. There, the sign of the offset is defined by the sign of the deviation of the center point potential. For control of the converter system by phase modulation functions the control of u_M can be performed in appropriate form by an offset of the zero-quantity (cf. p. 967 in [12]).

On the other hand, we have completely different conditions for DC-side optimum system operation ($i_{M,\mathrm{avg}} \to 0$). Here, the avoidance of low-frequency oscillations of u_M already is the ideal goal of the optimization. The symmetrization of the output partial voltages therefore can be realized simply by a highly dynamic control directly in connection with the optimization $i_{M,\mathrm{avg}} \to 0$.

7 Conclusions

In this paper the basic possibilities of an optimization of the operating behavior of three-phase three-level converter systems are considered. The optimization concerning the minimization of the stress on the output voltage center point by low-frequency current harmonics is compared to a minimization of the mains-side harmonic losses. There, for the sake of clearness the considerations are limited to purely resisitive behavior. The results are valid for unidirectional as well as for bidirectional three-level rectifier systems with high pulse frequency.

It becomes clear that for determination of a control method one has to always make a compromise between improvement of the DC-side/AC-side system behavior and the deterioration of the AC-side/DC-side system behavior. By a minimization of the oscillation of the center point potential the mains-side harmonic losses are increased. For the minimization of the mains-side harmonic losses there results a higher loading of the output voltage center point by low-frequency harmonics. Only the rms-value of the output capacitor current is not influenced by an optimization and shows (in a first approximation) a value which is only dependent on the mains current amplitude and on the modulation index! Furthermore, it becomes apparent that an even distribution $\rho_{--} = 0.5$ of the redundant switching states of the switching state sequences of each pulse period corresponds to a harmonic optimal operation with very good approximation.

In conclusion it appears, however, that for a practical realization of a three-level PWM rectifier system a DC-side optimal operation $i_{M,\mathrm{avg}} \to 0$ has to be preferred as compared to a minimization of the mains-side harmonic losses $\Delta^2_{N,\mathrm{rms}}$. If the output capacitors can be assumed to have an appropriate current carrying capability (in detail concerning the rms value of the current) one can reduce the capacitance which would otherwise be required for the limitation of the variation of the center point potential and/or the system power density can be increased. There, the mains-side harmonic losses are not increased significantly as compared to the optimal case. Thereby, approximately a globally optimum system behavior is obtained.

Acknowledgement

The authors are very much indebted to the *Hochschuljubiläumsstiftung der Stadt Wien* which generously supports the work of the Power Electronics Section at their university.

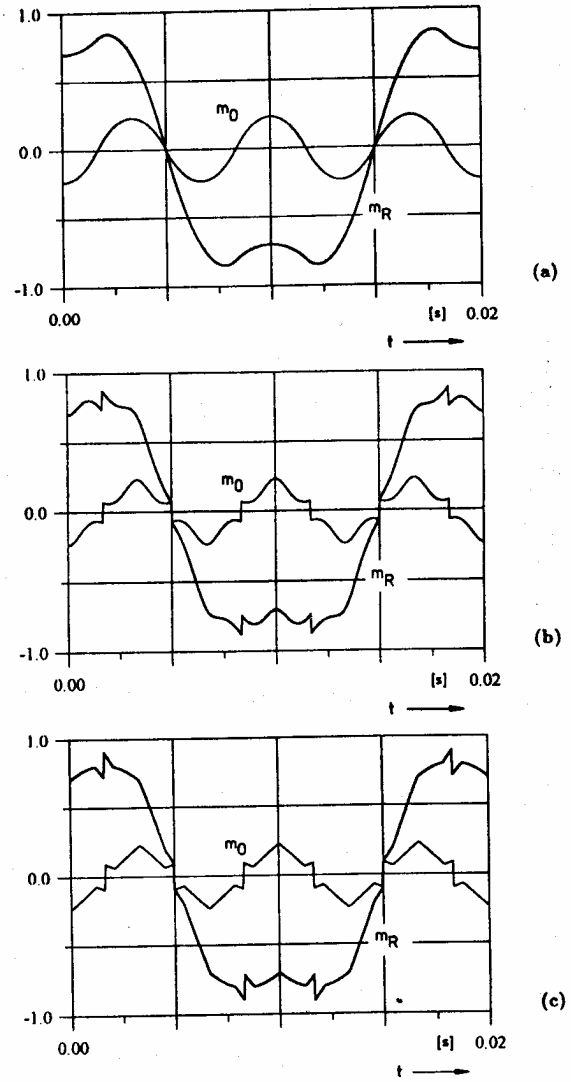

Fig.8: Time shape of the modulation function m_R and of the zero-quantity m_0 for $M = M_{(1)} = 0.93$ as related to the control methods (a), (b) and (c) according to Fig.6.

References

[1] **Holtz, J.:** *Selbstgeführte Wechselrichter mit treppenförmiger Ausgangsspannung für große Leistungen und hohe Frequenz.* Siemens Forschungs- und Entwicklungsberichte, Bd. 6, Nr. 3, S. 164–171 (1977).

[2] **Nabae, A., Takahashi, I., and Akagi, H.:** *A New Neutral-Point-Clamped PWM Inverter.* IEEE Transactions on Industry Applications, Vol. IA-17, No. 5, pp. 518–523 (1981).

[3] **Bhagwat, P.M., and Stefanovic, V.R.:** *Generalized Structure of a Multilevel PWM Inverter.* IEEE Transactions on Industry Applications, Vol. IA-19, No. 6, pp. 1057–1069 (1983).

[4] **Koczara, W., and Bialoskorski, P.:** *Multilevel Boost Rectifiers as a Unity Power Factor Supply for Power Electronics Drive and for Battery Charger.* Conference Proceedings of the IEEE International Symposium on Industrial Electronics, Budapest, June 1–3, pp. 477–481 (1993).

[5] **Zhao, Y., Li, Y., and Lipo, T.A.:** *Force Commutated Three-Level Boost Type Rectifier.* Conference Record of the 28th IEEE Industry Applications Society Annual Meeting, Toronto, Oct. 2–8, Pt. II, pp. 771–777 (1993).

[6] **Kolar, J.W., and Zach, F.C.:** *A Novel Three-Phase Three-Switch Three-Level PWM Rectifier.* Proceedings of the 28th Power Conversion Conference, Nürnberg, Germany, June 28–30, pp. 125–138 (1994).

[7] **Springmeier, F., and Steinke, J.K.:** *Control of the DC Link*

Neutral Potential of a Three-Level GTO Inverter as a Part of the Direkt Self Control (DSC). Proceeding of the 6th Conference on Power Electronics and Motion Control, Budapest, Hungary, Oct. 1–3, Vol.2, pp. 479–483 (1990).

[8] **Tadros, Y., Salama, S., and Höf, R.:** *Three-Level IGBT Inverter.* Proceedings of the 23rd IEEE Power Electronics Specialists Conference, Madrid, Spain, June 29 – July 3, Vol. I, pp. 46–52 (1992).

[9] **Kolar, J.W., and Zach, F.C.:** *A Novel Three-Phase Utility Interface Minimizing Line Current Harmonics of High-Power Telecommunications Rectifier Modules.* Record of the 16th IEEE International Telecommunications Energy Conference, Vancouver, Canada, Oct. 30– Nov. 3, pp. 367–374 (1994).

[10] **Fukuda, S., and Sagawa, A.:** *Modelling and Control of a Neutral-Point-Clamped Voltage Source Converter.* Proceedings of the International Power Electronics Conference, Yokohama, Japan, April 3–7, Vol. 1, pp. 470–475 (1995).

[11] **Rojas, R., Ohnishi, T., and Suzuki, T.:** *An Improved Vector Control Method for Neutral-Point-Clamped Inverters.* Proceedings of the IEEE Power Electronics Specialists Conference, Taipei, Taiwan R.O.C., June 20–25, Vol. II, pp. 951–957 (1994).

[12] **Ogasawara, S., and Akagi, H.:** *Analysis of Variation of Neutral Point Potential in Neutral-Point-Clamped Voltage Source PWM Inverters.* Proceedings of the 27th IEEE Industry Applications Society Annual Meeting, Toronto, Canada, Oct. 2–8, Pt. II, pp. 965–970 (1993).

[13] **Lee., Y.H., Suh, B.S., and Hyun, D.S.: :** *A Novel PWM Scheme for a Three-Level Voltage Source Inverter with GTO Thyristors.* Conference Record of the 29th IEEE Industry Applications Society Annual Meeting, Denver, Oct. 2–5, Vol. 2, pp. 1151–1157 (1994).

[14] **Miyashita, I., Kaku, B., and Sone, A.:** *A New PWM Method for 3-Level Inverter Based on Voltage Space Vector Suppressing the Neutral Point Potential Variation.* Proceedings of the International Power Electronics Conference, Yokohama, Japan, April 3–7, Vol. 1, pp. 506–511 (1995).

[15] **Liu, H.L., Choi, N.S., and Cho, G.H.:** *DSP Based Space Vector PWM for Three-Level Inverter with DC Link Voltage Balancing.* Proceedings of the 17th International Conference on Industrial Electronics, Control and Instrumentation, Kobe, Japan, Oct. 28– Nov. 1, Vol. 1, pp. 197–203 (1991)

[16] **Kolar, J.W., Drofenik, U., and Zach, F.C.:** *Current Handling Capability of the Neutral Point of a Three-Phase/Switch/Level Boost-Type PWM (VIENNA) Rectifier.* To be published at the IEEE Power Electronics Specialists Conference, Baveno, Italy, June 24–27 (1996).

[17] **Joetten, R., Gekeler, M., Eibel, J.:** *A.C. Drive with Three-Level Voltage Source Inverter and High Dynamic Performance Microprocessor Control.* Proceedings of the 1st European Conference on Power Electronics and Applications, Brussels, Belgium, Oct. 16–18, Vol. 2, pp. 3.1–3.6 (1985).

[18] **Velaerts, B., Mathys, P., and Zendaoui, Z.F.:** *Study of 2 and 3-Level Precalculated Modulations.* Proceedings of the 4th European Conference on Power Electronics and Applications, Firenze, Italy, Sept. 3–6, Vol. 3, pp. 228–234 (1991).

[19] **Halasz, S., Hassan, A.A.M., and Huu, B.T.:** *Optimal Control of Three Level PWM Inverters.* Proceedings of the 19th International Conference on Industrial Electronics, Control and Instrumentation, Lahaina, Maui, Hawaii, Nov. 15–19, Vol. 2, pp. 1228–1233 (1993).

[20] **Kolar, J.W., Ertl, H., and Zach, F.C.:** *Influence of the Modulation Method on the Conduction and Switching Losses of a PWM Converter System.* Conference Record of the 25th IEEE Industry Applications Society Annual Meeting, Seattle, WA, Oct. 7–12, Pt. 1, pp. 502–512 (1990). Also published in: IEEE Transaction on Industry Applications, Vol. IA-37, No. 6, pp. 1063–1075 (1991).

[21] **Holtz, J., Stadtfeld, S., and Lammert, P.:** *An Economic Very High Power PWM Inverter for Induction Motot Drives.* Proceedings of the 1st European Conference on Power Electronics and Applications, Brussels, Belgium, Oct. 16–18, Vol. 2, pp. 3.75–3.80 (1985).

[22] **Kolar, J.W., Drofenik, U., and Zach, F.C.:** *DC Link Voltage Balancing of Three-Phase/Switch/Level PWM (VIENNA) Rectifier by Modified Hysteresis Input Current Control.* Proceedings of the 30th International Power Conversion Conference, Nürnberg, Germany, June 20–22, pp. 443–465 (1995).

[23] **Kolar, J.W., Drofenik, U., and Zach, F.C.:** *Space Vector Based Analysis of the Variation and Control of the Neutral Point Potential of Hysteresis Current Controlled Three-Phase/Switch/Level PWM Rectifier Systems.* Proceedings of the International Conference on Power Electronics and Drive Systems, Singapore, Feb. 21–24, Vol.1, pp. 22–33 (1995).

[24] **Shimane, K., and Nakazawa, Y.:** *Harmonics Reduction for NPC Converter with a New PWM Scheme.* Proceedings of the International Power Electronics Conference, Yokohama, Japan, April 3–7, Vol. 1, pp. 482–487 (1995).

[25] **Klabunde, M.C., Zhao, Y., and Lipo, T.A.:** *Current Control of a 3-Level Rectifier/Inverter Drive System.* Conference Record of the 29th IEEE Industry Applications Society Annual Meeting, Denver, Oct. 2–5, Vol. 2, pp. 859–866 (1994).

[26] **Dahono, P. A., Sato, Y., and Kataoka, T.:** *Analysis of the Ripple Components of the Input Current and Voltage of PWM Converters.* Proceedings of the International Conference on Power Electronics and Drive Systems, Singapore, Feb. 21–24, Vol.1, pp. 323–328 (1995).

[27] **Kaźmierkowski, M.P., and Dzieniakowski, M. A.:** *Review of Current Regulation Methods for VS-PWM Inverters.* Conference Proceedings of the IEEE International Symposium on Industrial Electronics, Budapest, June 1–3, pp. 448–456 (1993).

[28] **Nagy, I.:** *Control Algorithm of a Three-Phase Voltage Sourced Reversible Rectifier.* Proceedings of the 4th European Conference on Power Electronics and Applications, Firenze, Italy, Sept. 3–6, Vol. 3, pp. 287–292 (1991).

[29] **Koczara, W.:** *Unity Power Factor Three-Phase Rectifier.* Proceedings of the 6th International (2nd European) Power Quality Conference, Munich, Oct. 14–15, pp. 79–88 (1992).

[30] **Jardan, K.R., Dewan, S.B., and Slemon, G.R.:** *General Analysis of Three-Phase Inverters.* IEEE Transactions on Industry and General Applications, Vol. IGA-5, No. 6, pp. 672–679 (1969).

[31] **Matakas Jr., L., and Masada, E.:** *Multi-Converter Implementation by Parallel Association of K Voltage Source Converters - Control Method.* Proceedings of the 5th European Conference on Power Electronics and Applications, Brighton, UK, Sept. 13–16, Vol. 4, pp. 35–40 (1993).

[32] **Salmon, J.C.:** *Circuit Topologies for PWM Boost Rectifiers Operated from 1-Phase and 3-Phase AC Supplies and Using Either Single or Split DC Rail Voltage Outputs.* Proceedings of the 10th IEEE Applied Power Electronics Conference, Dallas, TX, March 5–9, Vol.1, pp. 473–479 (1995).